This full text paper was peer reviewed at the direction of IEEE Communications Society subject matter experts for publication in the IEEE ICC 2010 proceedings

Exploiting Sink Mobility to Maximize Lifetime in 3D Underwater Sensor Networks

Shiqing Shen†, Andong Zhan†, Panlong Yang‡ and Guihai Chen†§
†State Key Laboratory for Novel Software Technology, Nanjing University, P. R. China
‡P.L.A University of Science and Technology, P. R. China
§Department of Computer Science, Shanghai Jiaotong University, P. R. China

Abstract—**Network lifetime is crucial to 3D Under Water Sensor Networks (UWSNs) because it decreases more seriously than in 2D scenarios as the radius of the monitored region grows. We utilize sink mobility to solve the problem intuitively because the sink deployed in a vehicle is controllable while sensors are hard to be retrieved and recharged. It is hard to extend the results in 2D scenarios, i.e., a circular motion, to 3D UWSNs directly because there are more factors influencing network lifetime. However there is little literature on utilizing and analyzing sink mobility in 3D UWSNs. To simplify 3D sink mobility, we convert any motion to a combination of circular motions through mapping. After discussing the characteristics of circular motions, we propose MOSS, an optimal MObile Sink Strategy, to maximize the network lifetime in 3D UWSNs. Simulation results show that MOSS outperforms other motion strategies and improves the network lifetime at least in the order of 800% when $R \geq 5r$, where R is the network radius and r is the transmission range of sensors.**

I. Introduction

Various architectures have been proposed for UWSN, which can be classified to 2D and 3D UWSNs. The former consist of UWSNs with sensor placed on the ocean floor [1] or floated on the ocean surface [2], while the latter include 3D UWSNs and sensor networks with AUVs (Automatic Underwater Vehicles [3]) mentioned in [1] and UWSNs composed of underwater and surface vehicles [4]. 3D UWSNs are used to detect and observe ocean phenomena that cannot be absolutely observed by bottom sensor nodes, e.g., to sample or monitor the 3D ocean environment.

The motivations of network lifetime prolongation in 3D underwater environments are:

1) the network lifetime, defined as the time when the first node runs out of energy, plays a crucial role in the performance of UWSNs, especially in 3D UWSNs. Even one sensor out of energy can have important effect on connectivity.
2) Since underwater sensors are hard to be retrieved and recharged, also solar energy cannot be exploited, we can use sink deployed in a vehicle to prolong network lifetime.

To solve these problems, our previous work [7] proposes an algorithm to utilize one extra AUV to prolong the network lifetime in 3D UWSNs. Here we present an alternative method to maximize the lifetime by exploiting sink mobility. The contributions of this paper include the following:

1) To the best of our knowledge, this paper is the first work to analyze sink motions in 3D UWSNs. We try to find where the node with the heaviest load is under single motion, then we propose MOSS which is a combination of single motions.
2) In Section 4, we use mapping to convert any sink motion to a combination of circle motions so that we can reduce the candidate solution space.
3) In Section 5, simulation results show that our optimal motion strategy outperforms other motion strategies. When $R = 5r$, it improves the lifetime in the order of 800%, and the lifetime increases as R increases.

The rest is organized as follows. Section 2 surveys related work. Section 3 describes UWSN model and the prolongation of the network lifetime. Section 4 presents mapping and proposes our optimal motion strategy. Section 5 gives simulation results in sparse underwater sensor networks. Finally, Section 6 concludes the paper.

II. Related Work

There has been intensive study in network lifetime prolongation by utilizing mobility for 2D terrestrial wireless sensor networks in the last few years. In [5], the authors exploit sink mobility for maximizing sensor networks lifetime and give a linear programming formulation for the joint problems of determining the movement of the sink and the sojourn time at different points. In [6], a joint mobility and routing strategy is proposed to improve lifetime by considering both sink mobility and multi-hop routing. In [8], the authors investigate the performance of a large dense network with one mobile relay and show that improvement in network lifetime over an all static network is upper bounded by a factor of four. The proof implies that the mobile relay needs to stay only within a two hop radius of the sink. They also propose a joint mobility and routing algorithm which comes close to the upper bound.

978-1-4244-6404-3/10/$26.00 ©2010 IEEE

Compared with terrestrial wireless sensor networks, motions of underwater nodes are more frequent and usually in a 3D underwater space. Literature [9] provides a method to estimate the battery lifetime and power cost of shallow water network and then uses this method to prolong the network lifetime for large networks by topology-dependent assignments. However, they do not consider nodes' mobility. Literature [10] proposes the meandering current mobility model in shadow water and analyzes its impact on underwater mobile sensor networks including network coverage and connectivity, nevertheless, without considering the active mobility of underwater sensors, e.g., AUVs. However, most former works of UWSNs ignore the impact of mobility on network lifetime in UWSNs.

Our former work [7] proposes an underwater aggregation routing algorithm UARA to prolong network lifetime by utilizing one AUV as one mobile relay for 3D sparse underwater sensor networks. In our present work, we first attempt to use the mobility of the sink to prolong the network lifetime in 3D underwater sensor networks.

III. Network Model And Problem Statement

A. Network Model

Underwater Sensor networks can be classified as 2D and 3D UWSNs. We focus only on 3D underwater sensor networks which can be used to perform cooperative sampling of the 3D ocean environments. The characteristics of underwater networks include their long distance of communication range, low transmission rate and their motions according to ocean currents. So underwater nodes (uw-nodes) are deployed sparsely and we can monitor a large space by making use of their motions. We assume that the network consists of n nodes and one mobile sink. The task of the mobile sink is to collect data from all nodes. The set of nodes is denoted as U. We are interested in communications between nodes and sink via either single hop or multi hop, whereas the communications between the sink and devices outside the network are out of the scope of this paper. Without loss of generality, we also assume the 3D space monitored is a hemisphere because the sink is deployed on the surface of the water and all other nodes are within a constant hop R from the sink node. The uw-nodes are deployed within R sparsely. We assume the density of nodes is the same within the space monitored.

B. Problem Statement

Since uw-nodes are deployed sparsely in 3D underwater environments, even when one node runs out of energy, it can have a deep impact on connectivity and coverage of the network. So we define network lifetime as the time span from the deployment to the time when the first uw-node runs out of energy. We assume all uw-nodes have the same initial energy while the sink has unlimited energy. The problems concerning the unequal initial energy are out of the scope of this paper. The load of node n, denoted as $load_n$, is the amount of energy consumed from when it is deployed underwater. The average load, referred as $\overline{load_n}$, is the average load of node n and its neighbors which are in its transmission range over a period. The routing protocol used here is based on shortest path routing. It is hard to get the expression of network lifetime, however we can convert this problem to a problem of load balancing, because the higher the load is, the shorter the network lifetime is. Therefore we formulate it as a min-max problem in terms of the average load of uw-node in 3D scenarios:

$$\begin{aligned} &Minimize \quad load_U = \max_{\forall n \in U} \overline{load_n}(strategies) \\ &Constraints: \quad subject\ to\ some\ strategies. \end{aligned}$$

Here strategies mean deterministic trajectory of the sink.

IV. Analysis of Sink Mobility in 3D Scenarios

In this section, first we derive the close form of $load_n$ in 3D scenarios, then we find an optimal place for static sink to achieve the longest network life. The result shows even when the sink is at its optimal position, the energy consumption is distributed unequally. In order to solve the energy unbalance problem, we make use of motions of the sink.

A. Close form of $load_n$ in 3D scenarios

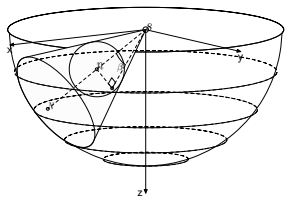

Fig. 1. Load Model

When we use a routing protocol based on shortest path routing, the following theorem is the expression of $load_n$:

Theorem 4.1:

$$\begin{aligned} \overline{load_n} &= \frac{(V_1+V_2)\rho\lambda\epsilon}{V_2\rho} \\ &\begin{cases} \approx & \frac{(\tan^2\beta L^3 - r^2 l)\lambda\epsilon}{2r^3} + \lambda\epsilon, & l \geq r\ , \\ = & \frac{R^3}{2r^3}\lambda\epsilon. & l < r \end{cases} \end{aligned}$$

where ρ is the mean density of uw-nodes, λ is the data rate to sink per node, and ϵ is the energy consumption per transmission. The sink is denoted as S and the uw-node as n, the intersection of line Sn and the surface of the hemisphere is N, l is the Euclidean distance of Sn and L is the Euclidean distance of SN, $\beta = \arcsin\frac{r}{l}$, is half of the conical angle as shown in Fig 1.

Proof: Here we adopt the assumption of energy consumption in our former work [7]. The energy consumption in idle state can be ignored and the transmit

energy cost is much larger than receive and sensing cost in underwater communications. According to the previous work [6] in 2D scenarios, when we use a routing protocol based on shortest path which is load balance, if the following conditions are satisfied, n_2 will forward data from n_1 to sink S: (i)the projection of n_2 on sn_1 is between S and n_1. (ii) the distance from n_2 to Sn_1 is less than w, which is set to be r here. In 3D scenario, to a given n_2, V_1 is the collection of all n_1s satisfying above conditions. Because the load are shared by n_2 and its neighbors within its transmission range towards S, let V_2 be the volume of this space, $\overline{load_n} = \frac{(V_1+V_2)\rho\lambda\epsilon}{V_2\rho}$. If Sn_2 is less than r, it is obvious V_1 is the whole hemisphere monitored, $\overline{load_n} = \frac{R^3}{2r^3}\lambda\epsilon$, otherwise, we denote the intersection of Sn_1 and the boundary of the 3D space as N_1, V_1 is the volume of part of the cone between n_1 and N_1, whose axis is sn_2, vertex is S and conical angle is 2β, $\overline{load_n} \approx \frac{(\tan^2\beta L^3 - r^2 l)\lambda\epsilon}{2r^3} + \lambda\epsilon$. ■

B. Optimal position for a static sink

Theorem 4.2: The optimal position for a static sink in terms of lowest energy consumption is the center$(0,0,0)$

Proof: If the sink is at somewhere not the center, there must be nodes more than R away from the sink. Meanwhile if the sink is at the center, all nodes are within R from the sink. In the former case, the energy unbalance of nodes near the sink is more serious, nodes near the sink runs out of energy earlier. So the optimal position is the center $(0,0,0)$ ■

However even when the sink is at its best position, the energy unbalance still exist, the nodes near the sink suffer heavy load, because they have to forward a great amount of traffic flows.

C. Analyzing motions of sink

To solve the problem of energy unbalance and get a lower $load_U$, we investigate different motions of the sink. Intuitively, if the sink moves, although the total energy consumption increases, it is dispersed among more uw-nodes. Consequently the following question is how the sink moves. Though there can be numerous motions, the following theorem guarantees that any irregular motion can be converted into a combination of circular motions whose center is at the z axis of the hemisphere and which is parallel with the horizontal level. However the $load_U$ after being converted is no more than the former.

Theorem 4.3: Any irregular motions of sink can be converted to a combination of circle motions whose $load_U$ is less than or equal to irregular motions.

Proof: Here we discuss only periodic irregular motions. Aperiodic motions can be seen as periodic motions whose period is the same as the network lifetime. The conversion is the same as in 2D scenarios except the motions rotate around the z axis of the hemisphere with an angle $\Delta\gamma$. Similarly when $\Delta\gamma \to 0$, the sink appears in the space formed by rotation with the same probability. The max load in irregular motion is denoted as $load_U^{ir}$, and the max load after conversion is referred as $load_U^{re}$. Considering an arbitrary node n, its load is$load_n^{re} = (2\pi)^{-1}\int_0^{2\pi} load_n^{\gamma} \mathrm{d}\gamma$, of course $load_n^{\gamma} \le load_U^{ir}$, so $load_n^{re} \le load_U^{ir}$. Because $load_U^{re} = \max_{\forall n\in U}\overline{load_n}$, $load_U^{re} \le load_U^{ir}$. ■

According to the above theorem, we just need to investigate the circle motions whose centers are at the z axis of the hemisphere. And we do not have to find the place whose *load* is the heaviest in the whole 3D space when sink moves around the z axis because of symmetry, we only have to find the place whose *load* is the heaviest in $Y = 0$ plane, and every node in the 3D space has a corresponding place in $Y = 0$ plane whose *load* is the same. Next we simplify our load model to analyze where the heaviest node is. The following theorems are two simplified load models, the former is a rough estimation and the latter is more accurate.

A rough estimation:

Corollary 4.1: $\overline{load_n} \approx \frac{(\frac{L^3}{l^2} - l)\lambda\epsilon}{2r} + \lambda\epsilon$

Proof: Here we simplify the general load model in Theorem 4.1, when $r \ll l$, we substitute $\tan\beta$ in Theorem 4.1, which equals $\tan\arcsin\frac{r}{l}$, with $\frac{r}{l}$. We get the simplified load model:

$\overline{load_n} \approx \frac{(\frac{L^3}{l^2} - l)\lambda\epsilon}{2r} + \lambda\epsilon.$ ■

A more accurate estimation when sink moves along a circle whose radius is R and whose center is $(0,0,0)$

Corollary 4.2: $\overline{load_n} \approx \int_0^{2\pi}(\frac{(\frac{lr^2L^3}{3\sqrt{l^2+r^2}} - l)\lambda\epsilon}{2r} + \lambda\epsilon)\mathrm{d}\theta$

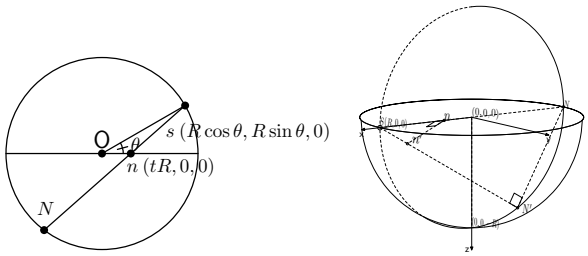

Fig. 2. A more accurate load model

Proof: First we will calculate the value of L and l. As shown in Fig. 2(a), sink S is at $(R\cos\theta, R\sin\theta, 0)$, $0 < \theta < 2\pi$ and node n is at $(tR, 0, 0)$, $0 < t < 1$. the intersection of line Sn and the circle is N, which is at $(R(\frac{2-2t\cos\theta}{1-2t\cos\theta+t^2}t + \frac{(t^2-1)\cos\theta}{1-2t\cos\theta+t^2}), R\sin\theta\frac{t^2-1}{1-2t\cos\theta+t^2}, 0)$. So l $(i.e., sn) = R\sqrt{1-2t\cos\theta+t^2}$ and L $(i.e., sN) = R\frac{2-2t\cos\theta}{\sqrt{1-2t\cos\theta+t^2}}$. Next we try to find a more accurate load model than the model in Corollary 4.1 which overestimates V_1 and somewhat ignores the effect of r. As shown in Fig. 2(b), $\triangle Snn' \simeq \triangle SN'N$, as $\angle n'Sn = \angle NSN'$ and $\angle n'nS = \angle SN'N$. We can derive that $NN' = \frac{r}{\sqrt{l^2+r^2}L}$, $SN' = \frac{l}{\sqrt{l^2+r^2}}L$ and $V_1 = \frac{1}{3}\pi\frac{lr^2L^3}{3\sqrt{l^2+r^2}} - \frac{1}{3}\pi r^2 l$. Because the sink is moving along the circle, we have to compute

the integral of θ on the interval $[0, 2\pi]$, i.e. $\overline{load_n} = \int_0^{2\pi} \frac{V_1(\theta)V_2(\theta)}{V_2(\theta)}\lambda\epsilon \mathrm{d}\theta$, $\overline{load_n} \approx \int_0^{2\pi}(\frac{(\frac{lr^2L^3}{3\sqrt{l^2+r^2}}-l)\lambda\epsilon}{2r} + \lambda\epsilon)\mathrm{d}\theta$ ■

Next we try to find properties of nodes in $Y = 0$ when sink moves along the circle whose center is at Z axis.

Lemma 4.4: When the sink moves along a circle parallel to the horizontal plane, whose center is $(0, 0, Z_S)$ and whose radius R_S is $\sqrt{R^2 - Z_S^2}$. For nodes at Z axis, whose z component is between $-R$ and Z_S, the *load* is the heaviest at $(0, 0, Z_S)$. For nodes at Z axis, whose z component is larger than Z_S, the *load* is the heaviest at the intersection of line $(R_S, 0, Z_S) - (-R_S, 0, 0)$ and Z axis, which is also the heaviest among nodes at the Z axis.

Proof: Let $(0, 0, z)$ be the position of an arbitrary node, $-R \le z \le Z_S$, it is obvious when z gets smaller, l gets larger and L gets smaller, and because these nodes are at the z axis, when sink moves, l and L keep constant.According to the load model in Corollary 4.1, when $z = Z_S$, the load is the heaviest. For nodes at Z axis whose z component is greater than Z_S, as z gets larger, l gets larger and $\frac{L}{l}$ gets larger, but when the intersection is at the $z = 0$ plane, $\frac{L}{l}$ gets smaller, so the heaviest load is at the intersection of line $(R_S, 0, Z_S) - (-R_S, 0, 0)$ and Z axis. ■

Lemma 4.5: When the sink moves along a circle whose center is $(0, 0, Z_S)$ and whose radius is $\sqrt{R^2 - Z_S^2}$. For nodes which are below $z = Z_S$ plane, there is a corresponding node in $z = Z_S$ plane whose load is heavier.

Proof: Let $R_S = \sqrt{R^2 - Z_S^2}$ be the radius of the circle. Let $(R_S, 0, Z_S)$ be the position of sink S. As shown in Fig.

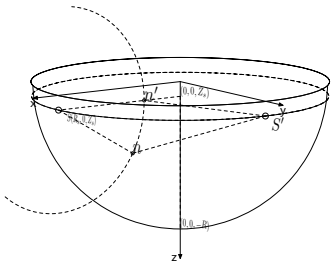

Fig. 3. Load comparison

3, the load of a node n in an arc of $Y = 0$ plane whose center is S and whose radius R' is less than R_S, is lighter than the load of the intersection n' of the arc and OS, which is at $(R_z - R', 0, Z_S)$.$N(N')$ is defined as the intersections of $Sn(Sn')$ and the hemisphere. It's obvious $Sn = Sn'$ and $SN > SN'$, according to Corollary 4.1, $load_n$ is heavier than $load'_n$. When sink moves, let $(R_S \sin\theta, R_S \cos\theta, Z_S)$ be the position of sink, $(R' \cos\alpha + R_S, 0, R' \sin\alpha + Z_S)$ be the position of an arbitrary node n and $(R_S - R', 0, Z_S)$ be the intersection n', $0 \le \theta \le 2\pi$, $\pi \le \alpha \le \frac{3}{2}\pi$, $R' \le R_S$. When $\alpha = \pi$, n is at the same position as n'. It's easy to derive $Sn = \sqrt{2(1 - \sin\theta)R_S^2 + R'^2 + 2R_S R'(1 - \sin\theta)\cos\alpha}$. This distance is an increasing monotonic function in $\pi \le \alpha \le \frac{3}{2}\pi$, so $Sn' \le Sn$ and it's easy to derive $SN' \ge SN$. According to Corollary 4.1, $load_{n'} \le load_n$. When $R_z < R' < 2R_z$, it's the same except the intersection is at the Z axis. According to Lemma 4.4, the loads of nodes on the arc whose radius is larger than R_S are lighter than the load of $(0, 0, Z_S)$. ■

According to Lemma 4.5, we only have to find the max load among nodes in the line $(0, 0, Z_S) - (R_S, 0, Z_S)$. Next we will show how to get the max load among nodes in the line $(0, 0, Z_S) - (R_S, 0, Z_S)$, according to the Corollary 4.2, the close form is too complicated to analyze, we compute the numerical integration of the accurate load model with $R = 5$,$r = 1$, other parameters are set to 1. The result shows that when $-1 < z < 0$, the load increases as the x components increases and when $-5 < z < -1$, the load decreases as the x components increases.

Theorem 4.6: when the sink moves at $z = Z_S$ plane, if the radius gets smaller, the max load will increase.

Proof: Let $S_1(r_1 \cos\theta, r_1 \sin\theta, Z_S)$, $S_2(r_2 \cos\theta, r_2 \sin\theta, Z_S)$ be two circles the sink moves at, $r_1 < r_2$. For nodes$(x, 0, Z_S)$ whose x component is less than r_1, $load_n^{S_1} > load_n^{S_2}$.(the indexes S_1,S_2 denote the different trajectory of the mobile sink.) Because $r_1 < r_2$, according to Theorem 4.1, $\beta^{S_1} > \beta^{S_2}$, and $nN^{S_1} = nN^{S_2}$, we derive that $V_1^{S_1} > V_1^{S_2}$ and $load_n^{S_1} > load_n^{S_2}$. It's trivial that nodes whose x component is less than r_1 bears more load than nodes whose x component is greater than r_1. If the load decreases as x increases, the node at the center of the circle has the heaviest load and when the radius of circle decreases, $load_U$ will increase. If the load increase as x increases, the close form of load is too complex to analyze, we use analytical result. As shown in Fig. 4, 5, 6, ($R = 5$, $r = 1$), the sink is moving at $z = 0$ plane with different radius 5, 4.5 and 2. The result shows that load of nodes in the decreased circle increases quickly, the max load still increase. ■

D. Mobile sink strategy (MOSS)

According to Theorem 4.6, when the sink is moving at $z = Z_S$ plane, the $load_U$ is minimal if the radius equals $\sqrt{R^2 - z^2}$. However if we use a strategy of combining different circles together, the $load_U$ will decrease because $load_U$ in different circle appears at different place. If we combine different circles together, load is scattered among nodes whose load is heavy under single circle. Here we adopt a heuristic combination, i.e., combining all the circles whose radius is $\sqrt{R^2 - z^2}$ when $z = Z_S$, from 0 to R, which is the surface of this hemisphere except the $z = 0$ plane. The sink is moving in this surface with the same probability. However in practice, our application is a data logging application, we assume the sink moves according to a predefined trajectory in the surface and uw-nodes know this trajectory, if not, there will be a lot of energy cost in broadcasting the location of the sink.

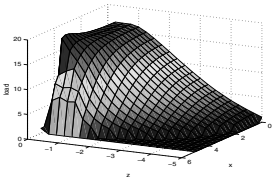

Fig. 4. load with $z = 0, R = 5$

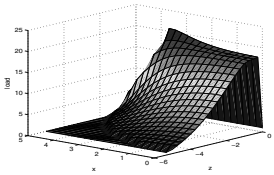

Fig. 5. load with $z = 0, R = 4.5$

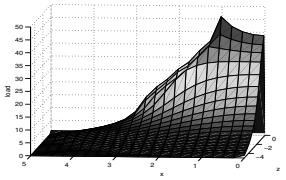

Fig. 6. load with $z = 0, R = 2$

V. Simulation Result

In our simulation, we consider the influences of different network radii and different speeds of the sink. We also compare the performance of MOSS with other strategies. In Fig. 7(a) and Fig. 7(b), all the lifetimes are normalized by setting the lifetime with static sink to 1, where the static sink is placed at *O*. *Random* shows the performance when the sink random walks in the hemisphere areas. *Circle* depicts the network lifetime when the sink rotates at the biggest circle. *MOSS* shows the network lifetime by using MOSS. *UARA* describes the performance of Underwater Aggregation Routing Algorithm [7] in different network sizes.

In Fig. 7(a), we set the speed of sink in all strategies to r per time unit, r is the transmission range. R is normalized by setting $r = 1$. Fig. 7(a) shows that with the increment of the network radius, the improvement of network lifetime by MOSS increases more markedly and rapidly than other strategies. When R is set to 5, MOSS can improve the lifetime about 8 times than when the sink is static. Furthermore, in order to investigate the influence of the speed of sink on different strategies, we test these mobile sink strategies by setting speed from $0.25r$ to $1.5r$ per time unit when network radius equals 5. Fig. 7(b) reveals that Random does not work well at a low speed, while speeds do not have a significant impact on the performance of Circle and MOSS.

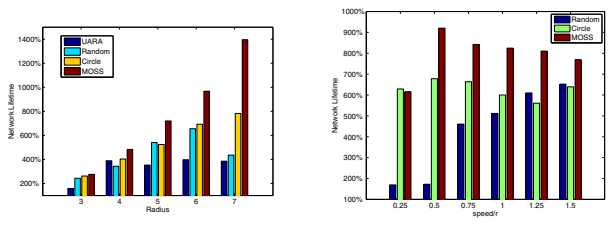

(a) (b)

Fig. 7. (a)The network lifetime comparison under different strategies. (b)The impact of different motion speed

VI. Conclusions

We first show that even when the sink is at its optimal position, some sensors run out of energy easily. It may have a deep impact on network connectivity and coverage of the UWSNs due to sparsely deployment. Thus we use sink mobility to solve this problem. We use mapping to convert any motion of the sink to a combination of circular motions. We reduce the solution space and only discuss the characteristics of circular motions. We further propose MOSS (an optimal MObility Sink Strategy). Compared with other motion strategies, MOSS works well and achieves a 800% improvement when $R = 5r$. In future work, we intend to combine sink mobility with different routing protocols in order to achieve a better result.

VII. Acknowledgment

The work is partly supported by China NSF grants (60721002, 60825205), China 863 project (2008AA01Z216, 2009AA01Z243) and China 973 project (2006CB303000, 2009CB3020402).

References

[1] I. F. Akyildiz, D. Pompili, and T. Melodia, "State-of-the-art in protocol research for underwater acoustic sensor networks," in *Proc. of WUWNet*, Los Angeles, CA, USA, Sept. 2006.

[2] E. Cayirci, H. Tezcan, Y. Dogan, and V. Coskun, "Wireless sensor networks for underwater surveillance systems," *Ad Hoc Networks*, vol. 4, no. 4, 2006.

[3] "Auv laboratory at mit sea grant." http://auvlab.mit.edu/.

[4] D. Pompili and I. F. Akyildiz, "Overview of networking protocols for underwater wireless communications," *IEEE Communications Magazine*, Jan. 2009.

[5] Z. M. Wang, S. Basagni, E. Melachrinoudis, and C. Petrioli, "Exploiting sink mobility for maximizing sensor networks lifetime," in *Proc. of the 38th Hawaii International Conference on System Sciences*, 2005.

[6] J. Luo and J. P. Hubaux, "Joint mobility and routing for lifetime elongation in wireless sensor networks," in *Proc. of the 24th IEEE INFOCOM*, mar 2005.

[7] A. Zhan, G. Chen, and W. Wang, "State-of-the-art in protocol research for underwater acoustic sensor networks," in *Proc. of ICCCN*, San Francisco, CA, USA, 2009.

[8] W. Wang, V. Srinivasan, and K. Chua, "Using mobile relays to prolong the lifetime of wireless sensor networks," in *Proc. of ACM Mobicom*, 2005.

[9] R. Jurdak, C. V. Lopes, and P. Baldi, "Battery lifetime estimation and optimization for underwater sensor networks," *Sensor Network Operations*, 2004.

[10] A. Caruso, F. Paparella, L. F. M. Vieira, M. Erol, and M. Gerla, "The meandering current mobility model and its impact on underwater mobile sensor networks," in *Proc. of IEEE INFOCOM*, 2008.

[11] J. Luo, D. Wang, and Q. Zhang, "Double mobility: Coverage of the sea surface with mobile sensor networks," in *Proc. of IEEE INFOCOM*, 2009.